Measurement and Calibration of Differential Mueller Matrix of Distributed Targets

Kamal Sarabandi, *Member, IEEE,* Yisok Oh, *Student Member, IEEE,* and Fawwaz T. Ulaby, *Fellow, IEEE*

Abstract—**The recent interest in radar polarimetry has led to the development of several calibration techniques to retrieve the Mueller matrix of a distributed target from the multipolarization backscatter measurements recorded by a radar system. Because a distributed target is regarded as a statistically uniform random medium, the measurements usually are conducted for a large number of independent samples (usually spatially independent locations), from which the appropriate statistics characterizing the elements of the Mueller matrix can be derived. Existing calibration methods rely on two major assumptions. The first is that the illuminated area of the distributed target is regarded as a single equivalent point target located along the antenna's boresight direction, and that the statistics of the scattering from all of the measured equivalent point targets (representing the spatially independent samples observed by the radar) are indeed the same as the actual scattering statistics of the distributed target. The second assumption pertains to the process by which the actual measurements made by the radar for a given illuminated area are transformed into the scattering matrix of that area. The process involves measuring the radar response of a point calibration target of known scattering matrix, located along the boresight direction of the antenna, and then modifying the measured response by a constant, known as the illumination integral, when observing the distributed target. The illumination integral accounts for only magnitude variations of the illuminating fields. Thus, possible phase variations or antenna crosstalk variations (between orthogonal polarization channels) across the beam are totally ignored, which may compromise the calibration accuracy. To rectify this deficiency of existing calibration techniques, a new technique is proposed with which the radar polarization distortion matrix is characterized completely by measuring the polarimetric response of a sphere over the entire main lobe of the antenna, rather than along only the boresight direction. Additionally, the concept of a "differential Mueller matrix" is introduced, and by defining and using a correlation–calibration matrix derived from the measured radar distortion matrices, the differential Mueller matrix is accurately calibrated. Comparison of data based on the previous and the new techniques shows significant improvement in the measurement accuracy of the copolarized and cross-polarized phase difference statistics.**

I. Introduction

THE literature contains a variety of different methods for measuring the backscattering cross section of point targets. In all cases, however, the calibration part of the measurement process involves a comparison of the measured radar response due to the unknown target with the measured response due to a calibration target of known radar cross section. Under ideal conditions, both the unknown and calibration targets are placed along the antenna boresight direction, thereby ensuring that both targets are subjected to the same illumination by the radar antenna. The situation is markedly different for distributed targets; the unknown distributed target is illuminated by the full antenna beam, whereas the calibration target—being of necessity a point target—is illuminated by only a narrow segment of the beam centered around the boresight direction. Consequently, both the magnitude and phase variations across the antenna pattern become part of the measurement process.

The magnitude variation usually is taken into account through a calculation of the illumination integral [1]–[4], but the phase variation has so far been ignored. The role of this phase variation across the beam with regard to polarimetric radar measurements and the means for taking it into account in the measurement process are the subject of this paper.

Terrain surfaces, including vegetation-covered and snow-covered ground, are treated as random media with statistically uniform properties. In radar measurements, the quantities of interest are the statistical properties of the scattered field per unit area. One such quantity is the scattering coefficient σ^o, which is defined in terms of the second moment of the scattered field:

$$\sigma^o = \lim_{r\to\infty} \lim_{A\to\infty} \frac{4\pi r^2}{A} \cdot \frac{\langle |E^s|^2 \rangle}{|E^i|^2}$$

where E^i and E^s are the incident and scattered fields, A is the illuminated area, and r is the range between the target area and the observation point. The above definition of σ^o is based on the assumption that the target is illuminated by a plane wave. Although in practice such a condition cannot be absolutely satisfied, it can be approximately satisfied under certain circumstances. The correlation length l of a distributed target represents the distance over which two points are likely to be correlated, implying that the currents induced at the two points due to an incident wave will likely be correlated as well. Thus, the correlation length may serve as the effective dimension of individual scatterers comprising the distributed target. The plane-wave approximation may be considered

Manuscript received February 6, 1992. This work was conducted under ARO Contract DAAL 03-91-G0202 and JPL Contract JPL-C-958749.

The authors are with the Radiation Laboratory, Department of Electrical Engineering and Computer Science, University of Michigan, Ann Arbor, MI 48109.

IEEE Log Number 9204943.

valid as long as the magnitude and phase variations of the incident wave are very small across a distance of several correlation lengths. In most practical situations, this "local" plane-wave approximation is almost always satisfied. When this is not the case, the measured radar response will depend on both the illumination pattern and the statistics of the distributed target [5], [6].

An implied assumption in the preceding discussion is that the phase variation across the antenna beam is the same for both the transmit and receive antennas. When making polarimetric measurements with dual-polarized transmit and receive antennas, the phase variation of the transmit and receive patterns may be different, which may lead to errors in the measurement of the scattering matrix of the target, unless the variations are known for all of the polarization combinations used in the measurement process and they are properly accounted for in the calibration process.

In this paper, we introduce a calibration procedure that accounts for magnitude and phase imbalances and antenna crosstalk across the entire main beam of the antenna. By applying this procedure, we can make accurate measurements of the differential Mueller matrix of a distributed target using the local plane-wave approximation. The differential Mueller matrix can then be used to compute the scattering coefficient for any desired combination of receive and transmit antenna polarizations, and by employing a recently developed technique [7], the statistics of the polarization phase differences can also be obtained. By way of illustrating the utility of the proposed measurement technique, we will compare the results of backscatter measurements acquired by a polarimetric scatterometer system for bare soil surfaces using the new technique with those based on calibrating the system with the traditional approach, which relies on measuring the response due to a calibration target placed along only the boresight direction of the antenna beam.

II. Theory

Consider a planar distributed target illuminated by a polarimetric radar system as shown in Fig. 1. Suppose the distributed target is statistically homogeneous and the antenna beam is narrow enough so that the backscattering statistics of the target can be assumed constant over the illuminated area. Let us subdivide the illumination area into a finite number of pixels, each including many scatterers (or many correlation lengths), and denote the scattering matrix of the ijth pixel by $\Delta\bar{\bar{S}}(x_i, y_j)$. The scattering matrix of each pixel can be considered as a complex random vector. If the radar system and its antenna are ideal, the scattered field associated with the ijth pixel is related to the incident field by

$$\begin{bmatrix} E_v^s \\ E_h^s \end{bmatrix} = K\frac{e^{2ik_0 r(x_i, y_j)}}{r(x_i, y_j)^2}\begin{bmatrix} \Delta S_{vv}(x_i, y_j) & \Delta S_{vh}(x_i, y_j) \\ \Delta S_{hv}(x_i, y_i) & \Delta S_{hh}(x_i, y_j) \end{bmatrix}\begin{bmatrix} E_v^i \\ E_h^i \end{bmatrix} \tag{1}$$

where E_v and E_h are the components of the electric field along two orthogonal directions in a plane perpendicular to the direction of propagation and K is a constant. In reality, radar systems are not ideal in the sense that the vertical and horizontal channels of the transmitter and receiver are not identical, and the radar antenna introduces some coupling between the vertical and horizontal signals at both transmission and reception. Consequently, the measured scattering matrix $\bar{\bar{U}}$ is related to the actual scattering matrix of a point target $\bar{\bar{S}}$ by [8]

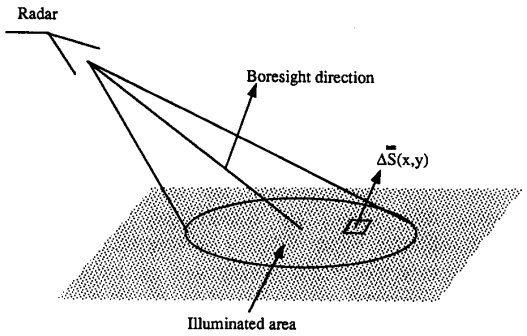

Fig. 1. Geometry of a radar system illuminating a homogeneous distributed target.

$$\bar{\bar{U}} = \frac{e^{2ik_0 r}}{r^2}\bar{\bar{R}}\bar{\bar{S}}\bar{\bar{T}} \tag{2}$$

where $\bar{\bar{R}}$ and $\bar{\bar{T}}$ are known as the receive and transmit distortion matrices. For small point targets where the illumination pattern of the incident field can be approximated by a uniform plane wave, measurement of $\bar{\bar{S}}$ is rather straightforward, and in recent years, this problem has been investigated thoroughly by many investigators [9]–[11]. The distortion matrices are obtained by measuring one or more targets of known scattering matrices, and then by inverting (2), the scattering matrix of the unknown target is obtained. In the case of distributed targets, however, distributed calibration targets do not exist. Moreover, the distortion matrices and the distance to the scattering points are all functions of position. That is, for the ijth pixel, the measured differential scattering matrix $\Delta\bar{\bar{U}}$ can be expressed by

$$\Delta\bar{\bar{U}} = \frac{e^{2ik_0 r(x_i, y_j)}}{r^2(x_i, y_j)}\bar{\bar{R}}(x_i, y_j) \cdot\begin{bmatrix} \Delta S_{vv}(x_i, y_j) & \Delta S_{vh}(x_i, y_j) \\ \Delta S_{hv}(x_i, y_j) & \Delta S_{hh}(x_i, y_j) \end{bmatrix}\bar{\bar{T}}(x_i, y_j). \tag{3}$$

The radar measures the sum of fields backscattered from all pixels within the illuminated area coherently, i.e.,

$$\bar{\bar{U}} = \sum_i \sum_j \frac{e^{2ik_0 r(x_i, y_j)}}{r^2(x_i, y_j)}\bar{\bar{R}}(x_i, y_j)\Delta\bar{\bar{S}}(x_i, y_j)\bar{\bar{T}}(x_i, y_j). \tag{4}$$

Thus, the measured scattering matrix is a linear function of the random scattering matrices of the pixels. For uniform distributed targets, we are interested in deriving information about the statistics of the differential scatter-

ing matrix from statistics of the measured scattering matrix $\bar{\bar{\mathbf{U}}}$. One step in relating the desired quantities to the measured ones is to perform a calibration procedure to remove the distortions caused by the radar and the antenna systems. The traditional approach used for calibrating polarimetric measurements of extended-area targets relies on two approximations. First, it is assumed that for each measured sample, the differential scattering matrix of the illuminated area is equal to some equivalent scattering matrix at boresight. Using this approximation, it is hoped that the equivalent scattering matrix has the same statistics as the original differential scattering matrix. This approximation is purely heuristic and cannot be justified mathematically. Second, the measured data for each sample are calibrated as if they were a point target, and the result is modified by a constant known as the illumination integral to account for the nonuniform illumination [3], [4]; thus, the crosstalk variations away from the antenna's boresight direction over the illuminated area are ignored. The illumination integral accounts for only magnitude variations of the gain patterns of the transmitter and receiver antennas, and no provision is made for accounting for any possible phase variations in the radiation patterns.

In this paper, we attempt to derive the second moments of the differential scattering matrix from the statistics of the measured matrix without making any approximation in the radar distortion matrices or using the equivalent differential scattering matrix representation. In random polarimetry, the scattering characteristics of a distributed target usually are represented by its Mueller matrix, which is the averaged Stokes matrix [4]. The Mueller matrix contains the second moments of the scattering matrix elements. By the central limit theorem, if the scatterers in the illuminated area are numerous and are of the same type, then the statistics describing the scattering are Gaussian (Rayleigh statistics). In such cases, knowledge of the Mueller matrix is sufficient to describe the scattering statistics of the target [7].

In a manner analogous with the definition of the scattering coefficient as the scattering cross section per unit area, let us define the differential Mueller matrix $\bar{\bar{\mathbf{M}}}^o$ as the ratio of the Mueller matrix ($\Delta\bar{\bar{\mathbf{M}}}$) derived from the differential scattering matrix ($\Delta\bar{\bar{\mathbf{S}}}$) to the differential area, i.e.,

$$\bar{\bar{\mathbf{M}}}^o = \lim_{\Delta A \to 0} \frac{\Delta \bar{\bar{\mathbf{M}}}}{\Delta A}.$$

To compute the differential Mueller matrix, the ensemble average of the cross products of the differential matrix components is needed. Let us define

$$\bar{\bar{\mathbf{W}}}^o = \begin{bmatrix} \langle S_{vv}^{o*} S_{vv}^o \rangle & \langle S_{vh}^{o*} S_{vh}^o \rangle & \langle S_{vh}^{o*} S_{vv}^o \rangle & \langle S_{vv}^{o*} S_{vh}^o \rangle \\ \langle S_{hv}^{o*} S_{hv}^o \rangle & \langle S_{hh}^{o*} S_{hh}^o \rangle & \langle S_{hh}^{o*} S_{hv}^o \rangle & \langle S_{hv}^{o*} S_{hh}^o \rangle \\ \langle S_{hv}^{o*} S_{vv}^o \rangle & \langle S_{hh}^{o*} S_{vh}^o \rangle & \langle S_{hh}^{o*} S_{vv}^o \rangle & \langle S_{hv}^{o*} S_{vh}^o \rangle \\ \langle S_{vv}^{o*} S_{hv}^o \rangle & \langle S_{vh}^{o*} S_{hh}^o \rangle & \langle S_{vh}^{o*} S_{hv}^o \rangle & \langle S_{vv}^{o*} S_{hh}^o \rangle \end{bmatrix} \tag{5}$$

where

$$\langle S_{pq}^{o*} S_{st}^o \rangle = \lim_{\Delta A \to 0} \frac{\langle \Delta S_{pq}^* \, \Delta S_{st} \rangle}{\Delta A}.$$

In terms of the correlation matrix $\bar{\bar{\mathbf{W}}}^o$, the differential Mueller matrix can be computed from

$$\bar{\bar{\mathbf{M}}}^o = 4\pi \nu \bar{\bar{\mathbf{W}}}^o \nu^{-1} \tag{6}$$

where [4]

$$\nu = \begin{pmatrix} 1 & 0 & 0 & 0 \\ 0 & 1 & 0 & 0 \\ 0 & 0 & 1 & 1 \\ 0 & 0 & -i & i \end{pmatrix}.$$

In order to calibrate a radar system so as to measure the differential Mueller matrix, let us represent each 2×2 matrix in (4) by a corresponding four-component vector, in which case (4) simplifies to

$$\bar{\mathscr{U}} = \sum_i \sum_j \frac{e^{2ik_0 r(x_i, y_j)}}{r^2(x_i, y_j)} \bar{\bar{\mathbf{D}}}(x_i, y_j) \, \overline{\Delta \mathscr{S}}(x_i, y_j) \tag{7}$$

where

$$\bar{\mathscr{U}} = \begin{bmatrix} U_{vv} \\ U_{vh} \\ U_{hv} \\ U_{hh} \end{bmatrix}, \qquad \overline{\Delta \mathscr{S}}(x_i, y_j) = \begin{bmatrix} \Delta S_{vv}(x_i, y_j) \\ \Delta S_{vh}(x_i, y_j) \\ \Delta S_{hv}(x_i, y_j) \\ \Delta S_{hh}(x_i, y_j) \end{bmatrix} \tag{8}$$

$$\bar{\mathscr{R}}(x_i, y_j) = \begin{bmatrix} R_{vv}(x_i, y_j) \\ R_{vh}(x_i, y_j) \\ R_{hv}(x_i, y_j) \\ R_{hh}(x_i, y_j) \end{bmatrix}, \qquad \bar{\mathscr{T}}(x_i, y_j) = \begin{bmatrix} T_{vv}(x_i, y_j) \\ T_{vh}(x_i, y_j) \\ T_{hv}(x_i, y_j) \\ T_{hh}(x_i, y_j) \end{bmatrix}$$

and it can be easily shown that

$$\bar{\bar{\mathbf{D}}}(x_i, y_j) = \begin{bmatrix} R_{vv}T_{vv} & R_{vv}T_{vh} & R_{vh}T_{vv} & R_{vh}T_{vh} \\ R_{vv}T_{hv} & R_{vv}T_{hh} & R_{vh}T_{hv} & R_{vh}T_{hh} \\ R_{hv}T_{vv} & R_{hv}T_{vh} & R_{hh}T_{vv} & R_{hh}T_{vh} \\ R_{hv}T_{hv} & R_{hv}T_{hh} & R_{hh}T_{hv} & R_{hh}T_{hh} \end{bmatrix}. \tag{9}$$

The mth component of the measured target vector ($\bar{\mathscr{U}}_m$) defined by (8) can be obtained from (7), and is given by

$$\mathscr{U}_m = \sum_i \sum_j \frac{e^{2ik_0 r(x_i, y_j)}}{r^2(x_i, y_j)} \left[\sum_{l=1}^{4} D_{ml}(x_i, y_j) \Delta \mathscr{S}_l(x_i, y_j) \right].$$

Thus, the averaged cross products of these components are

$$\begin{aligned} \langle \mathscr{U}_m \mathscr{U}_n^* \rangle = \sum_i \sum_j \sum_{i'} \sum_{j'} & \frac{e^{2ik_0[r(x_i, y_j) - r(x_{i'}, y_{j'})]}}{r^2(x_i, y_j) r^2(x_{i'}, y_{j'})} \\ & \cdot \sum_{l=1}^{4} \sum_{p=1}^{4} D_{ml}(x_i, y_j) D_{np}^*(x_{i'}, y_{j'}) \\ & \cdot \left\langle \Delta \mathscr{S}_l(x_i, y_j) \Delta \mathscr{S}_p^*(x_{i'}, y_{j'}) \right\rangle. \end{aligned} \tag{10}$$

If the number of scatterers in each pixel is assumed to be large, or the correlation length of the surface is much smaller than the pixel dimensions, then

$$\langle \Delta\mathscr{S}_l(x_i, y_j)\Delta\mathscr{S}_p^*(x_{i'}, y_{j'})\rangle = \begin{cases} 0, & i \neq i' \text{ and } j \neq j' \\ \langle \mathscr{S}_l^o \mathscr{S}_p^{o*}\rangle \Delta A_{ij}, & i = i' \text{ and } j = j'. \end{cases}$$

It should be mentioned here again that the target is assumed to be statistically homogeneous, and the antenna beam is assumed to have a narrow beam. Hence, $\langle \mathscr{S}_l^o \mathscr{S}_p^{o*}\rangle$ is not a function of position within the illuminated area. In the limit as ΔA approaches zero, (10) takes the following form:

$$\langle \mathscr{U}_m \mathscr{U}_n^*\rangle = \sum_{l=1}^{4}\sum_{p=1}^{4}\left[\int\int_A \frac{1}{r^4(x,y)} D_{ml}(x,y) \cdot D_{np}^*(x,y)\, dx\, dy\right]\langle \mathscr{S}_l^o \mathscr{S}_p^{o*}\rangle. \quad (11)$$

Equation (11) is valid for all combinations of m and n and, therefore, it constitutes 16 equations for the 16 correlation unknowns. Let us denote the measured correlations by a 16-component vector $\bar{\mathscr{Y}}$, and the actual correlations by another 16-component vector $\bar{\mathscr{X}}$ so that

$$\mathscr{X}_i = \langle \mathscr{S}_l^o \mathscr{S}_p^{o*}\rangle, \qquad i = 4(l-1) + p$$
$$\mathscr{Y}_j = \langle \mathscr{U}_m \mathscr{U}_n^*\rangle, \qquad j = 4(m-1) + n.$$

In this form, (11) reduces to the following matrix equation:

$$\bar{\mathscr{Y}} = \bar{\bar{\mathbf{B}}}\bar{\mathscr{X}} \quad (12)$$

where the ij element of $\bar{\bar{\mathbf{B}}}$ is given by

$$b_{ij} = \int\int_A \frac{1}{r^4(x,y)} D_{ml}(x,y) D_{np}^*(x,y)\, dx\, dy \quad (13)$$

and, as before,

$$i = 4(l-1) + p, \qquad j = 4(m-1) + n.$$

Once the elements of the correlation calibration matrix $\bar{\bar{\mathbf{B}}}$ are found from (13), (12) can be inverted to obtain the correlation vector $\bar{\mathscr{X}}$. The elements of the correlation vector are not arbitrary complex numbers; for example, $\mathscr{X}_2$ and $\mathscr{X}_5$ are complex conjugate of each other and $\mathscr{X}_1$ is a real number; thus, these relationships can be used as a criterion for calibration accuracy. The differential Mueller matrix can be obtained from the correlation matrix $\bar{\bar{\mathbf{W}}}^o$ whose entries in terms of the vector $\bar{\mathscr{X}}$ are given by

$$\bar{\bar{\mathbf{W}}}^o = \begin{bmatrix} \mathscr{X}_1 & \mathscr{X}_6 & \mathscr{X}_2 & \mathscr{X}_5 \\ \mathscr{X}_{11} & \mathscr{X}_{16} & \mathscr{X}_{12} & \mathscr{X}_{15} \\ \mathscr{X}_3 & \mathscr{X}_8 & \mathscr{X}_4 & \mathscr{X}_7 \\ \mathscr{X}_9 & \mathscr{X}_{14} & \mathscr{X}_{10} & \mathscr{X}_{13} \end{bmatrix}.$$

Evaluation of the elements of $\bar{\bar{\mathbf{B}}}$ requires knowledge of the radar distortion matrices over the main lobe of the antenna system. The distortion matrices of the radar can be found by applying the calibration method presented in the next section.

III. Calibration Procedure

As was shown in the previous section, the correlation vector $\bar{\mathscr{X}}$ can be obtained if the calibration matrix $\bar{\bar{\mathbf{D}}}(x, y)$ given by (9) is known. A simplified block diagram of a radar system is shown in Fig. 2. The quantities $\tilde{t}_v, \tilde{t}_h, \tilde{r}_v, \tilde{r}_h$ represent fluctuating factors of the channel imbalances caused by the active devices in the radar system. Without loss of generality, it is assumed that the nominal value of these factors is one, and their rate of change determines how often the radar must be calibrated. The antenna system also causes some channel distortion due to variations in the antenna pattern and path length differences. The crosstalk contamination occurs in the antenna structure, which is also a function of the direction of radiation. It has been shown that the antenna system, together with two orthogonal directions in a plane perpendicular to the direction of propagation, can be represented as a four-port passive network [8]. Using the reciprocity properties of passive networks, the distortion matrices of the antenna system were shown to be [8]

$$\bar{\bar{\mathscr{R}}}_a(\psi, \xi) = \begin{bmatrix} r_v(\psi,\xi) & 0 \\ 0 & r_h(\psi,\xi) \end{bmatrix}\begin{bmatrix} 1 & C(\psi,\xi) \\ C(\psi,\xi) & 1 \end{bmatrix} \quad (14)$$

$$\bar{\bar{\mathscr{T}}}_a(\psi, \xi) = \begin{bmatrix} 1 & C(\psi,\xi) \\ C(\psi,\xi) & 1 \end{bmatrix}\begin{bmatrix} t_v(\psi,\xi) & 0 \\ 0 & t_h(\psi,\xi) \end{bmatrix} \quad (15)$$

where ψ, ξ are some coordinate angles defined with respect to the boresight direction of propagation. The quantity $C(\psi, \xi)$ is the antenna crosstalk factor and $r_v(\psi, \xi), r_h(\psi, \xi), t_v(\psi, \xi), t_h(\psi, \xi)$ are the channel imbalances caused by the antenna system. These quantities are not subject to change due to variations in active devices, and once they are determined, they can be used repeatedly.

In order to find the radar distortion parameters at a given point (x, y) on the surface, we first need to specify a convenient coordinate system with respect to the antenna's boresight direction so that the distortions become independent of incidence angle and range to the target. The azimuth-over-elevation coordinate angles (ψ, ξ) provide a coordinate system that is appropriate for antenna pattern measurements. The angle ξ specifies the elevation angle and ψ specifies the azimuth angle in a plane with elevation ξ, as shown in Fig. 3. The mapping from (ψ, ξ) coordinates to (x, y) coordinates can be obtained by considering a radar at height h with incidence angle θ_0 and the boresight direction in the y–z plane, as shown in Fig. 4. It is easy to show that constant-ξ curves on the surface of a sphere map to constant-y lines and constant-ψ curves map to hyperbolic curves. The mapping functions are

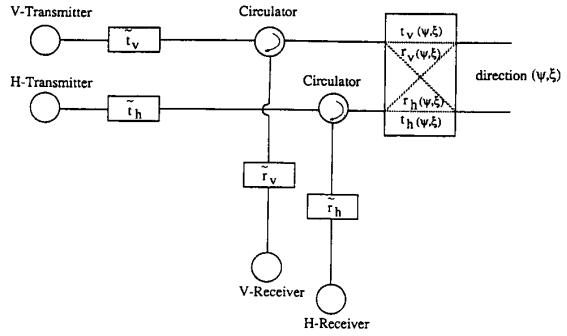

Fig. 2. Simplified block diagram of a polarimetric radar system.

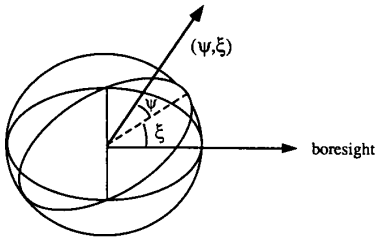

Fig. 3. Azimuth-over-elevation coordinate system (ψ, ξ) specifying a point on the surface of a sphere.

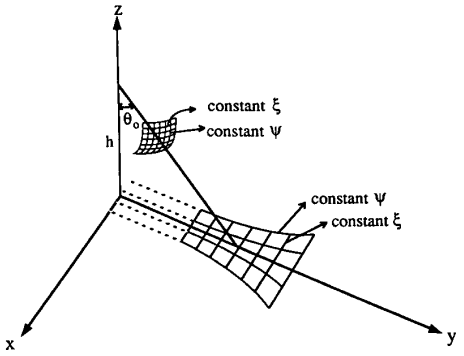

Fig. 4. Geometry of a radar above x–y plane and transformation of azimuth-over-elevation coordinate to Cartesian coordinate.

given by

$$x = \frac{h \tan \psi}{\cos(\theta_0 + \xi)}$$

$$y = h \tan(\theta_0 + \xi)$$

where $\psi = \xi = 0$ represents the boresight direction.

The entries of the calibration matrix $\overline{\overline{\mathbf{D}}}(\psi, \xi)$ as defined by (9) should be obtained through a calibration procedure. Following the single-target calibration technique given in [8], a single sphere is sufficient to determine the channel imbalances as well as the antenna crosstalk factor for a given direction. Hence, by placing a sphere with radar cross section σ^s at a distance r_0 and a direction (ψ, ξ) with respect to the radar, the receive and transmit distortion parameters can be obtained as follows:

$$R_{vv}T_{vv} = r_0^2 e^{-2ik_0 r_0} \frac{U_{vv}^s}{(1 + C^2)\sqrt{\sigma^s/4\pi}}$$

$$\beta \triangleq \frac{R_{hh}}{R_{vv}} = \frac{2C}{(1 + C^2)} \frac{U_{hh}^s}{U_{vh}^s}$$

$$\alpha \triangleq \frac{T_{hh}}{T_{vv}} = \frac{1 + C^2}{2C} \frac{U_{vh}^s}{U_{vv}^s}$$

$$C = \pm \frac{1}{\sqrt{a}}(1 - \sqrt{1 - a}) \tag{16}$$

where

$$a \triangleq \frac{U_{vh}^s U_{hv}^s}{U_{vv}^s U_{hh}^s}$$

and $\overline{\overline{\mathbf{U}}}^s$ is the measured (uncalibrated) response of the sphere at a specific direction (ψ, ξ). In terms of the known quantities given by (16), the calibration matrix $\overline{\overline{\mathbf{D}}}$ can be written as

$$\overline{\overline{\mathbf{D}}}(\psi, \xi) = R_{vv}T_{vv} \begin{bmatrix} 1 & C\alpha & C & C^2\alpha \\ C & \alpha & C^2 & C\alpha \\ C\beta & C^2\alpha\beta & \beta & C\alpha\beta \\ C^2\beta & C\alpha\beta & C\beta & \alpha\beta \end{bmatrix} \tag{17}$$

where the dependences on ψ and ξ of all parameters is understood.

In practice, it is impossible to measure the sphere for all values of ψ and ξ within the desired domain; however, by discretizing the domain of ψ and ξ (main lobe) into sufficiently small subdomains over which the antenna characteristics are almost constant, the integral given by (13) can be evaluated with good accuracy.

Polarimetric measurement of a sphere over the entire range of ψ and ξ is very time consuming, and under field conditions, performing these measurements seems impossible. However, this measurement can be performed in an anechoic chamber with the desired resolution $\Delta\psi$ and $\Delta\xi$ only once, and then under field conditions, we need to measure the sphere response only at boresight to keep track of variations in the active devices. Without loss of generality, let us assume that $\tilde{r}_v = \tilde{r}_h = \tilde{t}_v = \tilde{t}_h = 1$ for the sphere measurements when performed in the anechoic chamber, and that these quantities can assume other values for the measurements made under field conditions. If the measured distortion parameters at boresight (field condition) are denoted by prime and calculated from (16), then the channel imbalances corresponding to the field

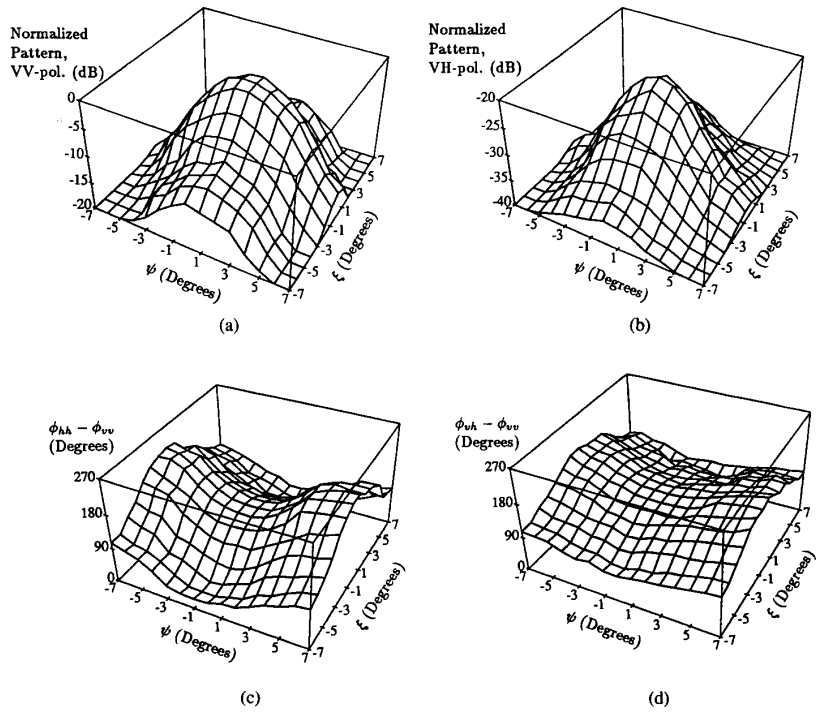

Fig. 5. Polarimetric response of a metallic sphere over the entire mainlobe of X-band scatterometer; normalized σ_{vv} (a) corresponds to G_v^2 and normalized σ_{vh} (b) corresponds to G_vG_h; phase difference between copolarized (c) and cross-polarized (d) components of the sphere response correspond to phase variation of the co- and cross-polarized patterns of the antenna.

measurements are

$$\tilde{r}_v\tilde{t}_v = \left(\frac{r_0'}{r_0}\right)^2 e^{-2ik_0(r_0'-r_0)}\frac{R'_{vv}(0,0)T'_{vv}(0,0)}{R_{vv}(0,0),T_{vv}(0,0)}$$
$$\frac{\tilde{t}_h}{\tilde{t}_v} = \frac{T'_{hh}(0,0)}{T'_{vv}(0,0)}\cdot\frac{T_{vv}(0,0)}{T_{hh}(0,0)}$$
$$\frac{\tilde{r}_h}{\tilde{r}_v} = \frac{R'_{hh}(0,0)}{R'_{vv}(0,0)}\cdot\frac{R_{vv}(0,0)}{R_{hh}(0,0)}. \quad (18)$$

Now, the calibration matrix at any direction ($\bar{\bar{\mathbf{D}}}'(\psi,\xi)$) can be obtained from (17) by replacing $R_{vv}T_{vv}$, α, and β by $R'_{vv}T'_{vv}$, α', and β' where

$$R'_{vv}T'_{vv} = \tilde{r}_v\tilde{t}_vR_{vv}T_{vv}$$
$$\alpha' = \frac{\tilde{t}_h}{\tilde{t}_v}\alpha$$
$$\beta' = \frac{\tilde{r}_h}{\tilde{r}_v}\beta. \quad (19)$$

Having found the calibration matrices for all subdomains, the element ij of the correlation–calibration matrix ($\bar{\bar{\mathbf{B}}}$), as given by (13), in the azimuth-over-elevation coordinate system takes the following form:

$$b_{ij} = \int\int_\Omega D_{ml}(\psi,\xi)D^*_{np}(\psi,\xi)\cdot\frac{\cos^2\psi\cos(\theta_0+\xi)}{h^2}\,d\psi\,d\xi \quad (20)$$

where Ω is the solid angle subtented by the illuminated area (main lobe of the antenna).

IV. Experimental Procedure and Comparison

To demonstrate the performance of the new calibration technique, the polarimetric response of a random rough surface was measured by a truck-mounted L-, C-, and X-band polarimetric scatterometer with center frequencies at 1.25, 5.3, and 9.5 GHz. Prior to these measurements, each scatterometer was calibrated in an anechoic chamber. The scatterometer was mounted on an azimuth-over-elevation positioner at one end of the chamber, and a 36 cm metallic sphere was positioned at the antenna boresight at a distance of 12 m. Then the polarimetric response of the sphere was measured over the mainlobe of the antenna. The sphere measurements at L-band, which has the widest beam of the three systems, was performed over $(\psi,\xi)\in[-21°,+21°]$ in steps of 3°, and the ranges of (ψ,ξ) for C- and X-band were $\pm10.5°$ and $\pm7°$ with steps of 1.5° and 1°, respectively. To improve the signal-to-noise ratio by removing the background contribution, the chamber in the absence of the sphere was also measured for all values of ψ and ξ.

Fig. 5(a) and (b) shows the co- and cross-polarized responses of the sphere at X-band, and Fig. 5(c) and (d) shows the co- and cross-polarized phase differences ($\phi_{hh}-\phi_{vv}$, $\phi_{hv}-\phi_{vv}$). Similar patterns were obtained for the L- and C-band. Using the sphere responses, the

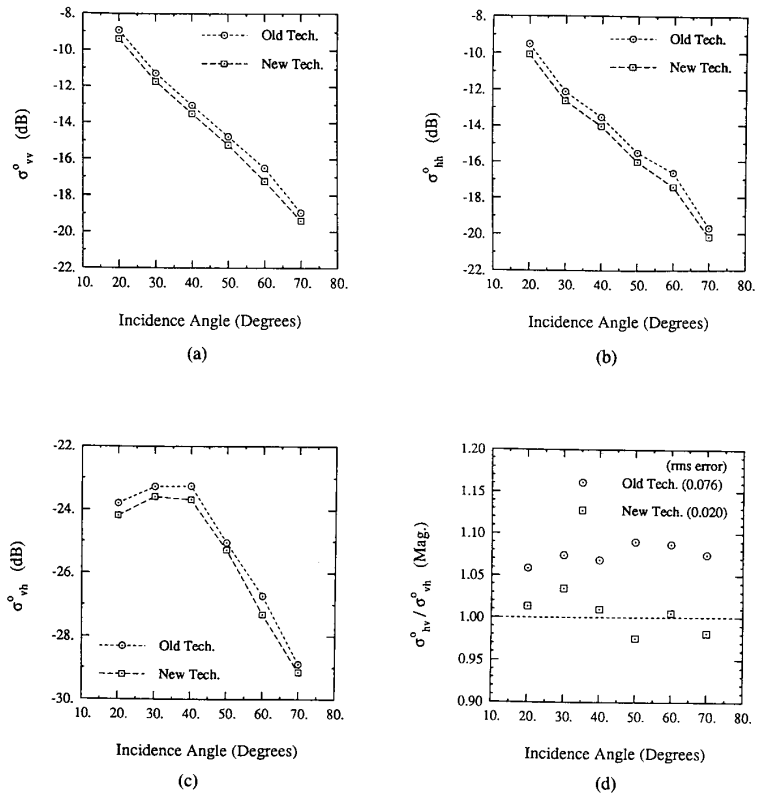

Fig. 6. Comparison between the new and old calibration techniques applied to the X-band measured backscatter from a bare soil surface. (a), (b), and (c) show the difference in the co- and cross-polarized backscattering coefficients, and (d) demonstrates the enhancement in the ratio of the cross-polarized backscattering coefficients obtained by the new method.

correlation–calibration matrices were determined as outlined in the previous section.

To evaluate the improvement provided by the new calibration technique, we shall compare results of polarimetric observations of a bare soil surface processed using the new technique with those obtained previously on the basis of the boresight-only calibration technique. The data were acquired from a truck-mounted 17-m-high platform for a rough surface with a measured rms height of 0.56 cm and a correlation length of 8 cm. The polarimetric backscatter response was measured as a function of incidence angle over the range 20°–70°. To reduce the effect of speckle on the measured data, 100 spatially independent samples were measured at each frequency and incidence angle. Also, the response of the sphere at the boresight was measured to account for any possible changes in the active devices. The collected backscatter data were calibrated by the new and old methods. The first test of accuracy of the new calibration algorithm was to make sure that the components of the correlation vector $\bar{\mathscr{X}}$ satisfy their mutual relationships, as explained in Section II. For all cases, these relationships were found to be valid within $\pm 0.05\%$.

The second step in the evaluation process is the relative comparison of the backscattering coefficients and phase statistics derived from the two techniques. Fig. 6(a)–(c) shows the co- and cross-polarized backscattering coefficients as a function of incidence angle, calibrated by the old and the new methods. The differences in backscattering coefficients, as shown in these figures, are less than 0.75 dB. It was found that the difference in backscattering coefficients is less than 1 dB for all frequencies and incidence angles. Although 1 dB error in σ° may seem negligible, in some cases, such as the variation with soil moisture content for which the total dynamic range of σ° is about 5 dB, the 1 dB error becomes significant. Fig. 6(d) shows the ratio of two cross-polarized scattering coefficients after calibration by each of the two methods. Theoretically, this ratio must be one and independent of incidence angle. In this figure, it is shown that the new calibration method more closely agrees with theoretical expectations than the old method.

The third step involves a comparison of the phase difference statistics of the distributed target. It has been shown that when the dimensions of the antenna footprint are much larger than the correlation length, the probability density function (pdf) of the phase differences can be expressed in terms of two parameters: the degree of correlation (α) and the polarized phase difference (ζ) [7]. The degree of correlation is a measure of the width of the

pdf, and the polarized phase difference represents the phase difference at which the pdf is maximum. These parameters can be computed directly from the components of the Mueller matrix and are given by [7]

$$\alpha = \frac{1}{2}\sqrt{\frac{(\mathcal{M}_{33}+\mathcal{M}_{44})^2 + (\mathcal{M}_{34}-\mathcal{M}_{43})^2}{\mathcal{M}_{11}\mathcal{M}_{22}}}$$

$$\zeta = \tan^{-1}\left(\frac{\mathcal{M}_{34}-\mathcal{M}_{43}}{\mathcal{M}_{33}+\mathcal{M}_{44}}\right).$$

Parameter α varies from zero to one, where zero corresponds to a uniform distribution and one corresponds to a delta-function distribution (fully polarized wave). Parameter ζ varies between $-180°$ and $180°$.

Fig. 7(a)–(c) shows the degree of correlation calculated by the new and old methods for the copolarized phase difference ($\phi_{hh} - \phi_{vv}$) at the L-, C-, and X-band, respectively. There is a significant difference between the two methods in all cases. The partially polarized backscattered Stokes vector obtained by the old calibration method appears more unpolarized than the Stokes vector obtained by the new method. The virtue of this result can be checked in the limiting case if an analytical solution is available. A first-order solution of the small perturbation method for slightly rough surfaces shows that the backscatter signal is fully polarized, and therefore, the pdf of the copolarized phase difference is a delta function, corresponding to $\alpha = 1$. The roughness parameters of the surface under investigation falls within the validity region of the small perturbation method at L-band. The value of α at L-band derived from the new calibration method is in much closer agreement with theoretical expectations than the value obtained by the old method. Fig. 8(a)–(c) shows plots of the copolarized phase difference at the L-, C-, and X-band, respectively. At the L- and X-bands, the value of ζ obtained by the two methods are positive and not very different from each other. Also, it noted that ζ has a positive slope with incidence angle. However, this is not the case for the C-band; the value of ζ obtained by the old method is negative, has a negative slope, while the behavior of ζ obtained by the new method is very similar to that at the other two frequencies. This deviation is due to the large variation of phase difference between the V- and H-channels of the C-band radar over the illumination area, and since the old method does not account for phase variations, it is incapable of correcting the resulting errors. Similar results were observed for the statistics of the cross-polarized phase difference ($\phi_{hv} - \phi_{vv}$).

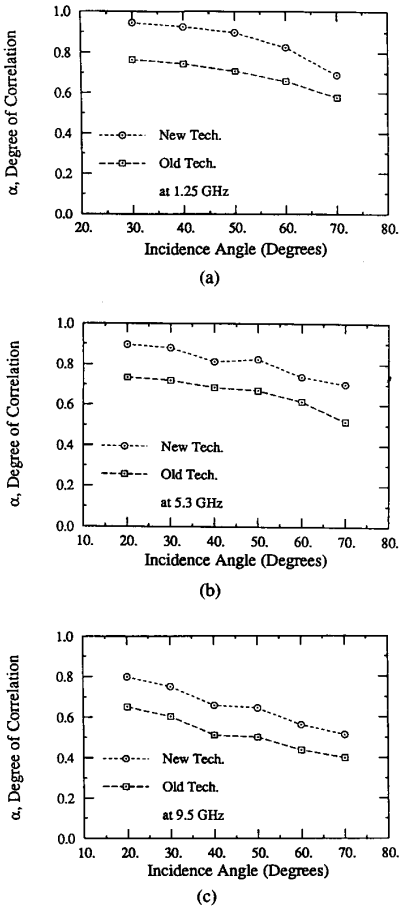

Fig. 7. Degree of correlation for copolarized components of the scattering matrix for the L-band (a), C-band (b), and X-band (c).

V. Conclusions

A rigorous method is presented for calibrating polarimetric backscatter measurements of distributed targets. By characterizing the radar distortions over the entire mainlobe of the antenna, the differential Mueller matrix is derived from the measured scattering matrices with a high degree of accuracy. It is shown that the radar distortions can be determined by measuring the polarimetric response of a metallic sphere over the main lobe of the antenna. The radar distortions are categorized into two groups, namely, distortions caused by the active devices, and distortions caused by the antenna structure (passive). Since passive distortions are immune to changes once they are determined, they can be used repeatedly. The active distortions can be obtained by measuring the sphere response only at boresight, thereby reducing the time required for calibration under field conditions. The calibration algorithm was applied to backscatter data collected from a rough surface by L-, C-, and X-band scatterometers. Comparison of results obtained with the new algorithm with the results derived from the old calibration method show that the discrepancy between the two methods is less 1 dB for the backscattering coefficients. The discrepancy, however, is more drastic for the phase-difference statistics, indicating that removal of the radar distortions from the cross products of the scattering matrix elements (differential Mueller matrix elements)

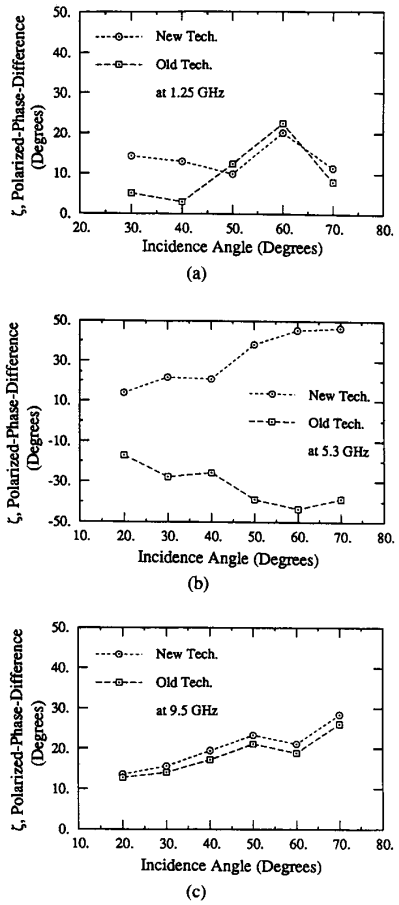

Fig. 8. Polarized phase difference for copolarized components of the scattering matrix for the L-band (a), C-band (b), and X-band (c).

cannot be accomplished with the traditional calibration methods.

REFERENCES

[1] F. T. Ulaby, R. K. Moore, and A. K. Fung, *Microwave Remote Sensing: Active and Passive, Vol. II—Radar Remote Sensing and Scattering Emission Theory*. Dedham, MA: Artech House, 1986.

[2] K. Sarabandi, Y. Oh, and F. T. Ulaby, "Polarimetric radar measurements of bare soil surfaces at microwave frequencies," in *Proc. IEEE Geosci. Remote Sensing Symp.*, Espoo, Finland, June 1991.

[3] M. A. Tassoudji, K. Sarabandi, and F. T. Ulaby, "Design consideration and implementation of the LCX polarimetric scatterometer (POLARSCAT)," Radiation Lab. Rep. 022486-T-2, Univ. Michigan, Ann Arbor, June 1989.

[4] F. T. Ulaby and C. Elachi, *Radar Polarimetry for Geoscience Applications*. Dedham, MA: Artech House, 1990.

[5] H. J. Eom and W. M. Boerner, "Rough surface incoherent backscattering of spherical wave," *IEICE Trans.*, vol. E 74, Jan. 1991.

[6] A. K. Fung and H. J. Eom, "Coherent scattering of spherical wave from an irregular surface," *IEEE Trans. Antennas Propagat.*, vol. AP-31, Jan. 1983.

[7] K. Sarabandi, "Derivation of phase statistics from the Mueller matrix," *Radio Sci.*, vol. 27, Sept.–Oct. 1992.

[8] K. Sarabandi and F. T. Ulaby, "A convenient technique for polarimetric calibration of radar systems," *IEEE Trans. Geosci. Remote Sensing*, vol. 28, Nov. 1990.

[9] R. M. Barnes, "Polarimetric calibration using in-scene reflectors," Rep. TT.65, M.I.T. Lincoln Lab., Lexington, MA, Sept. 1986.

[10] M. W. Whitt, F. T. Ulaby, P. Polatin, and V .V. Liepa, "A general polarimetric radar calibration technique," *IEEE Trans. Antennas Propagat.*, vol. 39, Jan. 1991.

[11] K. Sarabandi, F. T. Ulaby, and M. A. Tassoudji, "Calibration of polarimetric radar systems with good polarization isolation," *IEEE Trans. Geosci. Remote Sensing*, vol. 28, Jan. 1990.

Kamal Sarabandi (S'87–M'90) was born in Tehran, Iran, on November 4, 1956. He received the B.S. degree in electrical engineering from Sharif University of Technology, Tehran, Iran, in 1980. He entered the graduate program at the University of Michigan in 1984, and received the M.S.E. degree in electrical engineering in 1986, and the M.S. degree in mathematics and the Ph.D. degree in electrical engineering in 1989.

From 1980 to 1984 he worked as a Microwave Engineer in the Telecommunication Research Center in Iran. He is presently an Assistant Professor in the Department of Electrical Engineering and Computer Science, University of Michigan. His research interests include electromagnetic scattering, microwave remote sensing, and calibration of polarimetric SAR systems.

Dr. Sarabandi is a member of the Electromagnetics Academy and USNC/URSI Commission F.

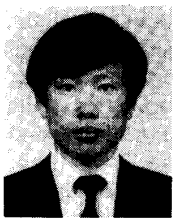

Yisok Oh (S'88) received the B.S. degree in electrical engineering from Yonsei University, Seoul, Korea, in 1982, and the M.S. degree in electrical engineering from the University of Missouri, Rolla, in 1988.

He is currently working towards the Ph.D. degree in electrical engineering at the University of Michigan, Ann Arbor, where he is a Research Assistant with the Radiation Laboratory. His research interests include microwave remote sensing, with an emphasis on the interface between experimental measurements and theoretical models for electromagnetic wave scattering from earth terrain.

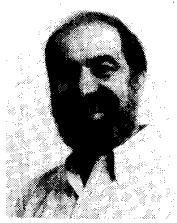

Fawwaz T. Ulaby (M'68–SM'74–F'80) received the B.S. degree in physics from the American University of Beirut, Lebanon, in 1964 and the M.S.E.E. and Ph.D. degrees in electrical engineering from the University of Texas, Austin, in 1966 and 1968, respectively.

He is currently a Professor of Electrical Engineering and Computer Science at the University of Michigan, Ann Arbor, and Director of the NASA Center for Space Terahertz Technology. His current interests include microwave and millimeter-wave remote sensing, radar systems, and radio wave propagation. He has authored several books and published over 400 papers and reports on these subjects.

Dr. Ulaby is the recipient of numerous awards, including the IEEE Geoscience and Remote Sensing Distinguished Achievement award in 1983, the IEEE Centennial Medal in 1984, the Kuwait Prize in Applied Science in 1986, and the NASA Achievement Award in 1990.